

# VLSI Implementation of a Pipelined 128 points 4-Parallel radix-2<sup>3</sup> FFT Architecture via Folding Transformation

James J. W. Kunst

jjwk89@gmail.com

Kevin H. Viglianco

kevinvig7@gmail.com

Daniel R. Garcia

dani6rg@gmail.com

Digital Signal Processing in Very Large Scale Integration Systems

Autumn 2019

Dr. Keshab K. Parhi

Dr. Ariel L. Pola

Universidad Nacional de Córdoba - FCEPyN

Av. Vélez Sársfield 1611, X5016GCA, Córdoba, Argentina

Fundación FULGOR

Ernesto Romagosa 518, Colinas V. Sarsfield, X5016GQN, Córdoba, Argentina

**Abstract—** In this work we present a develop and VLSI implementation of a 4-parallel pipelined architecture for the complex fast Fourier transform (CFFT) based on the radix-2<sup>3</sup> algorithm with 128 points using folding transformation and register minimization techniques. In addition, we are going to generate different synthesis levels from the hardware language description (HDL) with the purpose of obtaining a suitable performance on speed and area using standard cells at 45nm.

## I. INTRODUCTION

The Fast Fourier Transform (FFT) is widely used in different applications' fields, particularly, it is used in algorithms that involves apply digital signal processing, e.g., calculate the Discrete Fourier Transform (DFT) efficiently, that is useful because in some applications is most convenient to work in frequency domain than time domain. Nowadays is common utilize the algorithm of FFT for real time applications and parallel-pipelined hardware architecture give us the opportunity to work at high throughput rates.

There are two main types of pipelined FFT architectures [1]. On the one hand, feedback architectures (FB) which can be divided into Single-path Delay Feedback (SDF) and Multi-path Delay Feedback (MDF), these methods take out samples from each butterflies stages and feed back to the registers or memories at the same stage. On the other hand, feedforward architectures such as Multi-Path Delay Commutator (MDC) where the main difference with the feedback architectures is that SDF transfer data samples from one stage to other stage

serially, instead of that the MDC architecture transfer more than one sample per clock cycle and do not have feedback loops.

This work focuses on the design of 4-parallel pipelined architecture radix-2<sup>3</sup> 128-points for Complex FFT-DIF (Decimation in frequency). First, we will obtain the equations that correspond to Butterfly structure of radix-2<sup>3</sup> FFT-DIF for 8 points. After that, we apply these idea to design a 2-parallel pipelined architecture radix-2<sup>3</sup> 16-points FFT via folding transformation and find the appropriate rotators (*twiddles*) for each stage and clock cycle over the chain of butterflies on a feedforward architecture MDC. Second, we elaborate a float-point simulator which will process a summation of two cosine signals with different frequencies. Later, for the input and output of each stage of DFT, we quantized all operations such as adders and multipliers to get a fixed-point model. In this way, we can compare both models verifying the Signal to quantization noise ratio (SQNR) between fixed and float models.

Furthermore, we take the fixed-point model to elaborate our Synthesizable Verilog code HDL and verify the DFT functionality in each stage of the architecture. In addition to this, we generates power-area-timing report with different optimizations such as varying pipelining levels and canonical signed digit (CSD).

## II. THE RADIX-2<sup>3</sup> FFT ALGORITHM

The  $N$ -point DFT of an input sequence  $x[n]$  is defined as:

$$X[k] = \sum_{n=0}^{N-1} x[n] \cdot W_N^{nk}, \quad k = 0, 1, \dots, N-1 \quad (1)$$

$$\text{where } W_N^{nk} = e^{-j \frac{2\pi}{N} nk}$$

### III. DESIGN OF FFT ARCHITECTURE VIA FOLDING

In this section, we illustrate the folding transformation method to derive a 16-point DIF FFT 4-parallel architecture as an example and then, using the same method, we extend it to 128-point architecture. To do this, we will use the architecture proposed in [2].

#### A. 4-Parallel radix-2<sup>3</sup> 16-Points

In Fig. 1 we can see the flow graph of a 16-point DIF FFT radix-2. The graph is divided into four stages and each of them consist of a set of butterflies and multipliers. The twiddle factor in between the stages indicates a multiplication by  $W_N^k$ , where  $W_N$  denotes the  $N$ th root of unity, with its exponent evaluated modulo  $N$ . This can be represented as a DFG as shown in Fig. 2 where the nodes represents the butterfly computations of the radix-2 FFT algorithm.

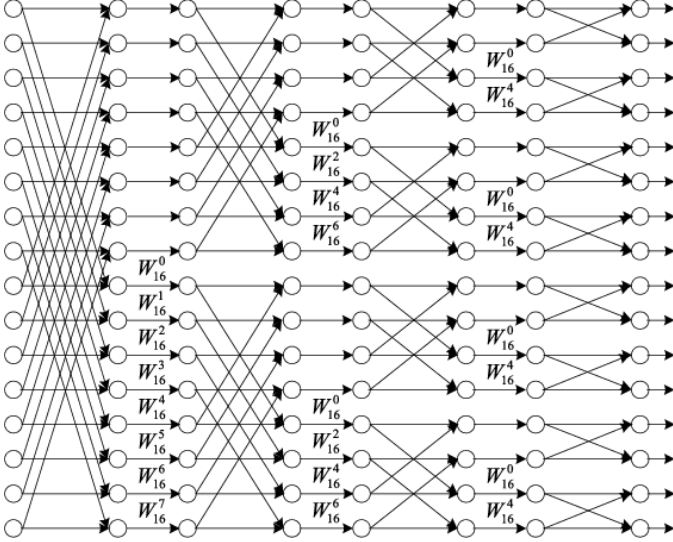


Figure 1: Flow graph of a radix-2 16-point DIF FFT.

The folding transformation is used on the DFG in to derive a pipelined architecture. To do this we need a folding set, which is an ordered set of operations executed by the same functional unit. Each folding set contains  $K$  entries, where  $K$  is called the folding factor. The operation in the  $j$ th position within the folding set (where goes from 0 to  $K-1$ ) is executed by the functional unit during the time partition. The term is called the folding order.

First we need to derive the folding equations, to do this consider an edge  $e$  connecting the nodes  $U$  and  $V$  with  $w(e)$  delays. Let the executions of the  $l$ th iteration of the nodes  $U$  and  $V$  be scheduled at the time units  $Kl + u$  and  $Kl + v$  respectively, where  $u$  and  $v$  are the folding orders of the nodes  $U$  and  $V$ , respectively. The folding equation for the edge  $e$  is:

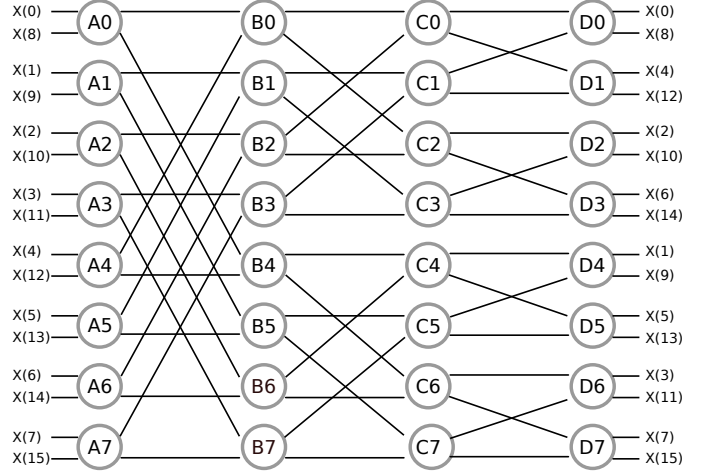


Figure 2: Data Flow graph (DFG) of a radix-2 16-point DIF FFT.

$$D_F(U \rightarrow V) = Kw(e) - P_U + v - u \quad (2)$$

where  $P_U$  is the number of pipeline stages in the hardware unit which executes the node  $U$ .

Consider folding of the the DFG in Fig. 2 with the folding sets:

$$\begin{aligned} A &= \{A0, A2, A4, A6\} & A' &= \{A1, A3, A5, A7\} \\ B &= \{B1, B3, B5, B7\} & B' &= \{B0, B2, B4, B6\} \\ C &= \{C2, C1, C3, C0\} & C' &= \{C6, C5, C7, C4\} \\ D &= \{D3, D0, D2, D1\} & D' &= \{D7, D4, D6, D5\} \end{aligned}$$

Assuming that the butterfly operations do not have any pipeline stages ( $P_A = P_B = P_C = P_D = 0$ ), the folding equations can be derived for all edges (see V-A1). For the folded system to be realizable,  $D_F(U \rightarrow V) \geq 0$  must hold for all the edges in the DFG. Retiming and/or pipeline can be applied to satisfy this property, if the DFG in Fig. 2 is pipelined/retimed as shown in Fig. 3 the system is realizable and the folded delays for the edges are given by V-A2.

We can see that the number of register required to implement the folding equations in V-A2 is 80. For minimize the number of registers we use the register minimization technique. If we let the output of node A1 be  $y_{(0)}$  and  $y_{(8)}$ , applying this successively with the rest of the nodes A we can obtain the linear life time chart for this stage in Fig. 4. Applying this criteria to the rest of the stages we can obtain the life time chart 5 and 6 for the outputs of the nodes B and C respectively, we can see that the numbers of maximum registers in each stage are 8, 4 and 8 respectively. More information about this method can be found on [3].

The register allocation tables for each of lifetime charts are shown in Fig. 7, 8 and 9 respectively, we can implement the same equations in V-A2 using 20 registers with register minimization techniques. The folded architecture in Fig. 10 is synthesized using the folding equations and the register allocation tables, the method can be found in [3].

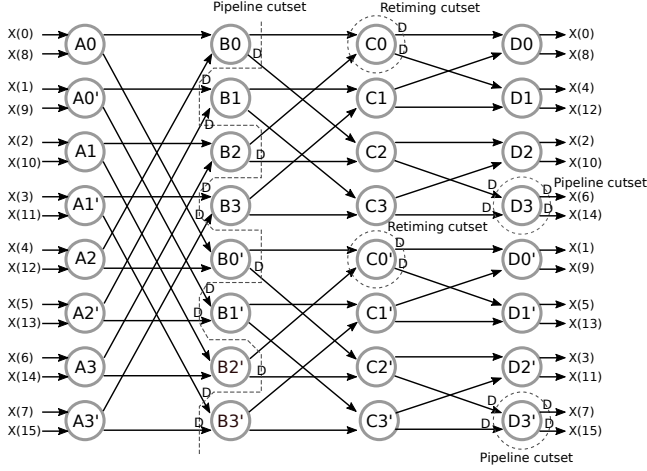


Figure 3: Data Flow graph (DFG) of a radix-2 16-point DIF FFT with retiming and pipeline.

	I/P	R1	R2	R3	R4	R5	R6	R7	R8
0	y <sub>0</sub> ,y <sub>8</sub> ,y <sub>1</sub> ,y <sub>9</sub>								
1	y <sub>2</sub> ,y <sub>10</sub> ,y <sub>3</sub> ,y <sub>11</sub>	y <sub>1</sub>		y <sub>0</sub>		y <sub>9</sub>		y <sub>8</sub>	
2	y <sub>4</sub> ,y <sub>12</sub> ,y <sub>5</sub> ,y <sub>13</sub>	y <sub>3</sub>	y <sub>1</sub>	y <sub>2</sub>	y <sub>0</sub>	y <sub>11</sub>	y <sub>9</sub>	y <sub>10</sub>	y <sub>8</sub>
3	y <sub>6</sub> ,y <sub>14</sub> ,y <sub>7</sub> ,y <sub>15</sub>	y <sub>5</sub>	y <sub>3</sub>	y <sub>1</sub>	y <sub>2</sub>	y <sub>13</sub>	y <sub>11</sub>	y <sub>9</sub>	y <sub>10</sub>
4		y <sub>7</sub>	y <sub>5</sub>	y <sub>3</sub>	y <sub>1</sub>	y <sub>15</sub>	y <sub>13</sub>	y <sub>11</sub>	y <sub>9</sub>
5			y <sub>7</sub>		y <sub>3</sub>		y <sub>15</sub>		y <sub>11</sub>

Figure 4: Linear lifetime chart for the variables  $y_0, y_1, \dots, y_{15}$  for a 16-point FFT architecture.

	I/P	R1	R2	R3	R4
2	z <sub>0</sub> ,z <sub>4</sub> ,z <sub>8</sub> ,z <sub>12</sub>				
3	z <sub>2</sub> ,z <sub>6</sub> ,z <sub>10</sub> ,z <sub>14</sub>	z <sub>4</sub>	z <sub>0</sub>	z <sub>12</sub>	z <sub>8</sub>
4	z <sub>1</sub> ,z <sub>5</sub> ,z <sub>9</sub> ,z <sub>13</sub>	z <sub>6</sub>	z <sub>4</sub>	z <sub>14</sub>	z <sub>12</sub>
5	z <sub>3</sub> ,z <sub>7</sub> ,z <sub>11</sub> ,z <sub>15</sub>	z <sub>5</sub>	z <sub>1</sub>	z <sub>13</sub>	z <sub>9</sub>
6		z <sub>7</sub>	z <sub>5</sub>	z <sub>15</sub>	z <sub>13</sub>

Figure 5: Linear lifetime chart for the variables  $z_0, z_1, \dots, z_{15}$  for a 16-point FFT architecture.

	I/P	R1	R2	R3	R4	R5	R6	R7	R8
4	w <sub>0</sub> ,w <sub>2</sub> ,w <sub>8</sub> ,w <sub>10</sub>								
5	w <sub>4</sub> ,w <sub>6</sub> ,w <sub>12</sub> ,w <sub>14</sub>	w <sub>2</sub>		w <sub>0</sub>		w <sub>10</sub>		w <sub>8</sub>	
6	w <sub>1</sub> ,w <sub>3</sub> ,w <sub>9</sub> ,w <sub>11</sub>	w <sub>6</sub>	w <sub>2</sub>	w <sub>4</sub>	w <sub>0</sub>	w <sub>14</sub>	w <sub>10</sub>	w <sub>12</sub>	w <sub>8</sub>
7	w <sub>5</sub> ,w <sub>7</sub> ,w <sub>13</sub> ,w <sub>15</sub>	w <sub>3</sub>	w <sub>6</sub>	w <sub>2</sub>	w <sub>4</sub>	w <sub>11</sub>	w <sub>14</sub>	w <sub>10</sub>	w <sub>12</sub>
8		w <sub>7</sub>	w <sub>3</sub>	w <sub>6</sub>	w <sub>2</sub>	w <sub>15</sub>	w <sub>11</sub>	w <sub>14</sub>	w <sub>10</sub>
9			w <sub>7</sub>		w <sub>6</sub>		w <sub>15</sub>		w <sub>14</sub>

Figure 6: Linear lifetime chart for the variables  $w_0, w_1, \dots, w_{15}$  for a 16-point FFT architecture.

The inputs of each folding node are represented with a matrix where the values in the same column are data that flow in parallel and values in the same row flow through the same path in consecutive clock cycles. The first two rows represents the inputs of the superior BF and the others two represents the input of the inferior BF. The same criteria is used for represent the constants of rotators, where each number  $k$  of the matrix represent a multiplication by  $W_N^k$ .

As we can see in 10, we suppose that the inputs and output are not ordered, to order these variables extra logic are needed, using more registers and multiplexers.

The different types of rotators used in Fig. 10 are shown in Fig. 11, the description of each of them can be found below.

- Trivial rotator: They can be carried out by interchanging the real and imaginary components and/or changing the sign of the data.
- Constant CSD rotator: They can be carried out by interchanging the real and imaginary components and/or a multiplication by a unique constant fractional number, in this case we will use a CSD multiplier to perform the area utilized.
- General rotator: They can be carried out by interchanging the real and imaginary components and/or a multiplication by more than one constant fractional numbers, in this case we will use a general multiplier.

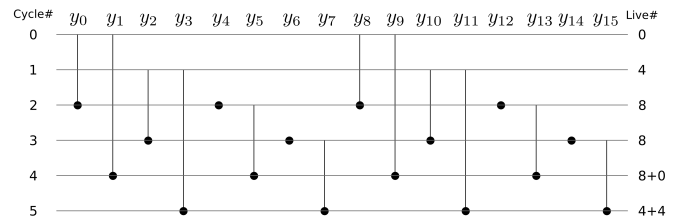


Figure 7: Register allocation table for the data represented in 4

#### B. 4-Parallel radix-2<sup>3</sup> 128-Points

We can deduce the folding architecture following the same method than used with the 4-Parallel radix-2<sup>3</sup> 16-Points. The DFG and folding set used can be shown in Fig. ?? and Fig. I in V-C and V-B.

The architecture can be seen in Fig. 12

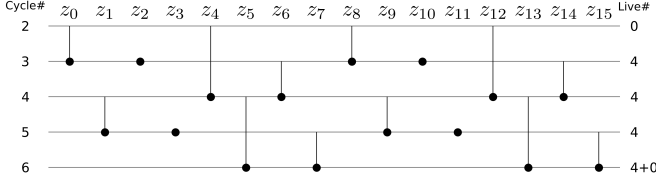


Figure 8: Register allocation table for the data represented in 5

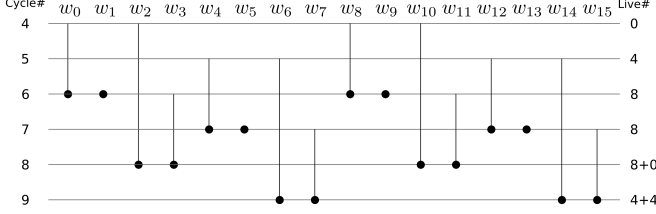


Figure 9: Register allocation table for the data represented in 6

#### IV. IMPLEMENTATION

#### V. CONCLUSION

#### APPENDIX

##### A. Folding equations for 16-points FFT

###### 1) Without retimming:

$D_F(D0 \rightarrow B0) = 2$	$D_F(D0 \rightarrow B4) = 2$
$D_F(D1 \rightarrow B1) = 0$	$D_F(D1 \rightarrow B5) = 0$
$D_F(D2 \rightarrow B2) = 2$	$D_F(D2 \rightarrow B6) = 2$
$D_F(D3 \rightarrow B3) = -1$	$D_F(D3 \rightarrow B7) = -1$
$D_F(D4 \rightarrow B0) = 0$	$D_F(D4 \rightarrow B4) = 0$
$D_F(D5 \rightarrow B1) = -1$	$D_F(D5 \rightarrow B5) = -1$
$D_F(D6 \rightarrow B2) = 0$	$D_F(D6 \rightarrow B6) = 0$
$D_F(D7 \rightarrow B3) = -2$	$D_F(D7 \rightarrow B7) = -2$
$D_F(E0 \rightarrow C0) = 1$	$D_F(E0 \rightarrow C2) = -2$
$D_F(E1 \rightarrow C1) = 1$	$D_F(E1 \rightarrow C3) = 2$
$D_F(E2 \rightarrow C0) = 0$	$D_F(E2 \rightarrow C2) = -3$
$D_F(E3 \rightarrow C1) = 0$	$D_F(E3 \rightarrow C3) = 1$
$D_F(E4 \rightarrow C4) = 1$	$D_F(E4 \rightarrow C6) = -2$
$D_F(E5 \rightarrow C5) = 1$	$D_F(E5 \rightarrow C7) = 2$
$D_F(E6 \rightarrow C4) = 0$	$D_F(E6 \rightarrow C6) = -3$
$D_F(E7 \rightarrow C5) = 0$	$D_F(E7 \rightarrow C7) = 1$
$D_F(F0 \rightarrow D0) = -2$	$D_F(F0 \rightarrow D1) = 0$
$D_F(F1 \rightarrow D0) = 0$	$D_F(F1 \rightarrow D1) = 2$
$D_F(F2 \rightarrow D2) = 2$	$D_F(F2 \rightarrow D3) = 0$
$D_F(F3 \rightarrow D2) = 0$	$D_F(F3 \rightarrow D3) = -2$
$D_F(F4 \rightarrow D4) = -2$	$D_F(F4 \rightarrow D5) = 0$
$D_F(F5 \rightarrow D4) = 0$	$D_F(F5 \rightarrow D5) = 2$
$D_F(F6 \rightarrow D6) = 2$	$D_F(F6 \rightarrow D7) = 0$
$D_F(F7 \rightarrow D6) = 0$	$D_F(F7 \rightarrow D7) = -2$

###### 2) With retimming:

$D_F(D0 \rightarrow B0) = 2$	$D_F(D0 \rightarrow B4) = 2$
$D_F(D1 \rightarrow B1) = 4$	$D_F(D1 \rightarrow B5) = 4$
$D_F(D2 \rightarrow B2) = 2$	$D_F(D2 \rightarrow B6) = 2$
$D_F(D3 \rightarrow B3) = 3$	$D_F(D3 \rightarrow B7) = 3$
$D_F(D4 \rightarrow B0) = 0$	$D_F(D4 \rightarrow B4) = 0$
$D_F(D5 \rightarrow B1) = 3$	$D_F(D5 \rightarrow B5) = 3$
$D_F(D6 \rightarrow B2) = 0$	$D_F(D6 \rightarrow B6) = 0$
$D_F(D7 \rightarrow B3) = 2$	$D_F(D7 \rightarrow B7) = 2$
$D_F(E0 \rightarrow C0) = 1$	$D_F(E0 \rightarrow C2) = 2$
$D_F(E1 \rightarrow C1) = 1$	$D_F(E1 \rightarrow C3) = 2$
$D_F(E2 \rightarrow C0) = 0$	$D_F(E2 \rightarrow C2) = 1$
$D_F(E3 \rightarrow C1) = 0$	$D_F(E3 \rightarrow C3) = 1$
$D_F(E4 \rightarrow C4) = 1$	$D_F(E4 \rightarrow C6) = 2$
$D_F(E5 \rightarrow C5) = 1$	$D_F(E5 \rightarrow C7) = 2$
$D_F(E6 \rightarrow C4) = 0$	$D_F(E6 \rightarrow C6) = 1$
$D_F(E7 \rightarrow C5) = 0$	$D_F(E7 \rightarrow C7) = 1$
$D_F(F0 \rightarrow D0) = 2$	$D_F(F0 \rightarrow D1) = 4$
$D_F(F1 \rightarrow D0) = 0$	$D_F(F1 \rightarrow D1) = 2$
$D_F(F2 \rightarrow D2) = 2$	$D_F(F2 \rightarrow D3) = 4$
$D_F(F3 \rightarrow D2) = 0$	$D_F(F3 \rightarrow D3) = 2$
$D_F(F4 \rightarrow D4) = 2$	$D_F(F4 \rightarrow D5) = 4$
$D_F(F5 \rightarrow D4) = 0$	$D_F(F5 \rightarrow D5) = 2$
$D_F(F6 \rightarrow D6) = 2$	$D_F(F6 \rightarrow D7) = 4$
$D_F(F7 \rightarrow D6) = 0$	$D_F(F7 \rightarrow D7) = 2$

##### B. Folding set used in 4-parallel radix-2<sup>3</sup> 128-points

##### C. Pipelined DFG of a 128-point DIF FFT

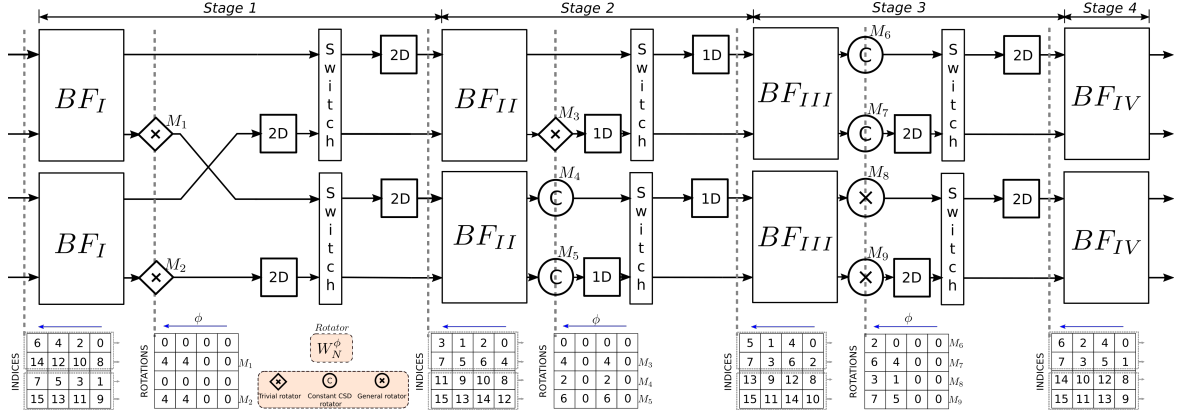


Figure 10: Folding architecture for the computation of a radix-2<sup>3</sup> 16-point DIF complex FFT.

A	A0	A2	A4	A6	A8	A10	A12	A14	A16	A18	A20	A22	A24	A26	A28	A30
A'	A32	A34	A36	A38	A40	A42	A44	A46	A48	A50	A52	A54	A56	A58	A60	A62
B	B1	B3	B5	B7	B9	B11	B13	B15	B17	B19	B21	B23	B25	B27	B29	B31
B'	B0	B2	B4	B6	B8	B10	B12	B14	B16	B18	B20	B22	B24	B26	B28	B30
C	B33	B35	B37	B39	B41	B43	B45	B47	B49	B51	B53	B55	B57	B59	B61	B63
C'	B32	B34	B36	B38	B40	B42	B44	B46	B48	B50	B52	B54	B56	B58	B60	B62
D	C16	C18	C20	C22	C24	C26	C28	C30	C1	C3	C5	C7	C9	C11	C13	C15
D'	C17	C19	C21	C23	C25	C27	C29	C31	C0	C2	C4	C6	C8	C10	C12	C14
E	C48	C50	C52	C54	C56	C58	C60	C62	C33	C35	C37	C39	C41	C43	C45	C47
E'	C49	C51	C53	C55	C57	C59	C61	C63	C32	C34	C36	C38	C40	C42	C44	C46
F	D8	D10	D12	D14	D16	D18	D20	D22	D24	D26	D28	D30	D1	D3	D5	D7
F'	D9	D11	D13	D15	D17	D19	D21	D23	D25	D27	D29	D31	D0	D2	D4	D6
G	D40	D42	D44	D46	D48	D50	D52	D54	D56	D58	D60	D62	D33	D35	D37	D39
G'	D41	D43	D45	D47	D49	D51	D53	D55	D57	D59	D61	D63	D32	D34	D36	D38
H	E4	E6	E8	E10	E12	E14	E16	E18	E20	E22	E24	E26	E28	E30	E1	E3
H'	E5	E7	E9	E11	E13	E15	E17	E19	E21	E23	E25	E27	E29	E31	E0	E2
I	E36	E38	E40	E42	E44	E46	E48	E50	E52	E54	E56	E58	E60	E62	E33	E35
I'	E37	E39	E41	E43	E45	E47	E49	E51	E53	E55	E57	E59	E61	E63	E32	E34
J	F2	F4	F6	F8	F10	F12	F14	F16	F18	F20	F22	F24	F26	F28	F30	F1
J'	F3	F5	F7	F9	F11	F13	F15	F17	F19	F21	F23	F25	F27	F29	F31	F0
K	F34	F36	F38	F40	F42	F44	F46	F48	F50	F52	F54	F56	F58	F60	F62	F33
K'	F35	F37	F39	F41	F43	F45	F47	F49	F51	F53	F55	F57	F59	F61	F63	F32
L	G3	G5	G7	G9	G11	G13	G15	G17	G19	G21	G23	G25	G27	G29	G31	G0
L'	G2	G4	G6	G8	G10	G12	G14	G16	G18	G20	G22	G24	G26	G28	G30	G1
M	G35	G37	G39	G41	G43	G45	G47	G49	G51	G53	G55	G57	G59	G61	G63	G32
M'	G34	G36	G38	G40	G42	G44	G46	G48	G50	G52	G54	G56	G58	G60	G62	G33

Table I: Folding set for the DFG showed in Fig. ??

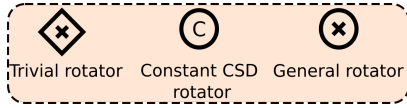


Figure 11: Symbols used for the different types of rotators

## REFERENCES

- [1] Shousheng He and M. Torkelson, "Designing pipeline FFT processor for OFDM (de)modulation," in *1998 URSI International Symposium on Signals, Systems, and Electronics. Conference Proceedings (Cat. No.98EX167)*. IEEE, pp. 257–262. [Online]. Available: <http://ieeexplore.ieee.org/document/738077/>
- [2] M. Ayinala, M. Brown, and K. K. Parhi, "Pipelined Parallel FFT Architectures via Folding Transformation," *IEEE Transactions on Very Large Scale Integration (VLSI) Systems*, vol. 20, no. 6, pp. 1068–1081, Jun. 2012. [Online]. Available: <http://ieeexplore.ieee.org/document/5776727/>
- [3] K. K. Parhi, *VLSI Digital Signal Processing Systems. Design and implementation*. JOHN WILEY & SONS, INC., 1999, pp. 157–163.

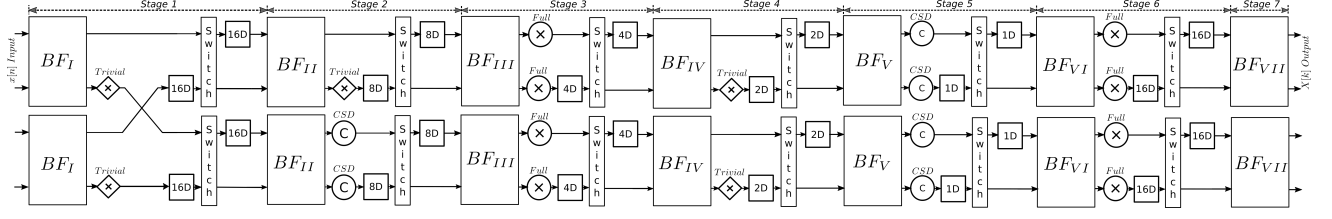


Figure 12: Folding architecture for the computation of a radix-2<sup>3</sup> 128-point DIF complex FFT.

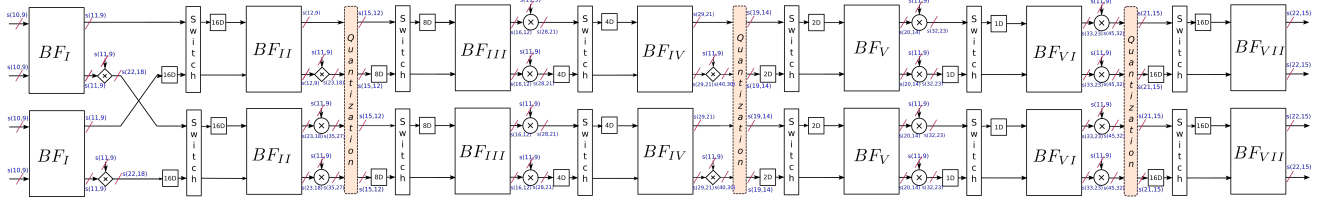


Figure 13

